Lectures and Workshop International
- Recent Advances in Multidisciplinary Technology and Modeling -
May 23rd-25th, 2007

Aeroelastic Control of Composite Plate Wings based on the Optimal Placement of Sensors and Actuators

Masaki KAMEYAMA

Department of Aerospace Engineering, Tohoku University
6-6-01, Aramaki-Aza-Aoba, Aoba-ku, Sendai 980-8579, JAPAN

Abstract

The present paper treats the flutter suppression of composite plate wings with segmented piezoelectric sensors and actuators. First, fundamental mechanism of flutter suppression based on the measurement and control of specific vibration modes is examined for composite plate wings. Aeroelastic analysis of composite plates is based on the finite element method and the subsonic unsteady lifting surface theory. Polyvinylidene fluoride (PVDF) sensors are used as a modal sensor for measurement of specific modal displacements, which is constructed by optimizing the sensor gain distribution. Lead zirconate titanate (PZT) actuators are also used as actuators for flutter suppression, which generate the modal forces for specific modes with the pseudo-optimal output feedback control law based on the linear quadratic regulator (LQR) control theory. The importance of the measurement and control of the first torsional vibration mode for the flutter suppression is clarified through the numerical examples.

Next, validity of the flutter suppression based on the optimal placement of a limited number of sensors and actuators is examined for composite plate wings. Modal sensor for measurement of the modal displacement of the first torsional vibration mode is designed by the optimal placement of PVDF sensors based on the minimization criterion of observation spillover. Actuation system to generate the modal force for the first torsional vibration mode is designed by the optimal placement of PZT actuators based on the minimization criterion of control spillover. The effectiveness of optimal placement of sensors and actuators in the flutter suppression is clarified through the numerical examples.

I. Introduction

Aeroelastic characteristics have played the significant role in structural design of aircraft wing. Flutter is one of the representative dynamic phenomena of aeroelastic instability, which results in catastrophic destruction of wing structures. For the improvement of flutter property, active control technology with respect to aeroelastic response by using sensors and actuators has also been studied [1-3] since a flutter suppression system was demonstrated by using B-52E airplane in 1970s. Recently, it has been widely accepted that active aeroelastic control technology is the important one related to safety and weight reduction of aircraft structures for future research and development on aircraft in Japan [4]. On the other side, numerous research and development on the active control technology have been carried out as the fundamental one in order to realize so-called morphing aircraft in the United States, for example the Smart Wing program by Defense Advanced Research Projects Agency (DARPA) and the Active Aeroelastic Wing flight research program by the U.S. Air Force Research Laboratory (AFRL), NASA Dryden Flight Research Center (DFRC), and Boeing Phantom Works.

Studies on aeroelastic control technology have been carried out by adopting several kinds of structural, aerodynamic and control models, although, they can be classified into two groups by sort of sensors and actuators to be used for measurement and control; aeroelastic control with control surfaces and with smart materials. Smart structures that control their aeroelastic response by using built-in sensors and actuators have drawn attention of many researchers [5,6]. Especially, a lot of research on the application of piezoelectric materials [7] to flutter control has been carried out, since piezoelectric materials are effective on active control in

high frequency region from the viewpoint of quick response. It should be noted that the present study has focused on piezoelectric materials as smart materials for a control device, not shape memory materials from the same point of view mentioned above.

The unsettled problems of current research in these fields can be classified in accordance with the following aspects: it is indicated that feedback control based on the measurement and control of torsional vibration is effective on flutter suppression of two-dimensional airfoil with trailing-edge control surface through the previous numerical investigations on fundamental mechanism of flutter suppression. To the authors' best knowledge, however, all of the previous studies have not yet investigated the effects of feedback control with respect to specific vibration modes on flutter suppression of three-dimensional wings, like a plate wing, in detail. On the other side, various kinds of more sophisticated robust control rules have been mainly adopted for the flutter suppression of three-dimensional lifting surface, like a plate wing, and the validity of the proposed control methods has been examined through the numerical and experimental results. However, design methods of measurement and control system for flutter suppression considering the importance of the feedback control with respect to specific vibration modes have not yet been examined.

The present paper treats the flutter suppression of composite plate wings with segmented piezoelectric sensors and actuators. First, fundamental mechanism of flutter suppression based on the measurement and control of specific vibration modes is examined for unswept composite plate wings. Aeroelastic analysis of composite plates is based on the finite element method and the subsonic unsteady lifting surface theory. Piezoelectric sensors are used as a modal sensor for measurement of specific modal displacements, which is constructed by optimizing the sensor gain distribution. Piezoelectric actuators are also used as actuators for flutter suppression, which generate the modal forces for specific modes with the pseudo-optimal output feedback control law based on the LQR control theory. The importance of the measurement and control of the first torsional vibration mode for the flutter suppression is clarified through the numerical examples.

Next, validity of the flutter suppression based on the optimal placement of a limited number of piezoelectric sensors and actuators is examined for unswept composite plate wings. Modal sensor for measurement of the modal displacement of the first torsional vibration mode is designed by the optimal placement of piezoelectric sensors based on the minimization criterion of observation spillover. Actuation system to generate the modal force for the first torsional vibration mode is designed by the optimal placement of piezoelectric actuators based on the minimization criterion of control spillover. The effectiveness of optimal placement of sensors and actuators in the flutter suppression is clarified through the numerical examples.

II. Fundamental Equations

A. Aeroelastic Response of Composite Plate Wings with Segmented Piezoelectric Sensors and Actuators

The finite element equations for aeroelastic response of cantilevered laminated plates with piezoelectric patches can be described as follows:

$$\begin{aligned} &[M]\{\ddot{w}\}+[K]\{w\}=q[Q]\{w\}-[A]\{\phi_A\}, \\ &\{\phi_S\}=-[S]\{w\}, \end{aligned} \tag{1}$$

where the mass matrix is denoted by M, the displacement vector is denoted by w and the dynamic pressure is denoted by q. The aerodynamic influence matrix is denoted by Q. In this paper, the aerodynamic influence matrix Q, which represents the unsteady aerodynamic forces acting on the vibratory wing surface in subsonic flow, is evaluated based on the doublet-point method [8]. Besides, the matrices K, A and S can be described as follows:

$$\begin{aligned} &[K]=[K_{ww}]-[K_{w\phi}][K_{\phi\phi}]^{-1}[K_{\phi w}], \\ &[A]=[K_{w\phi}],\ [S]=[K_{\phi\phi}]^{-1}[K_{\phi w}], \end{aligned} \tag{2}$$

where the elastic stiffness matrix is denoted by K_{ww}, the mechanical-electric coupling stiffness matrices are denoted by $K_{w\phi}$ and $K_{\phi w}$, and the piezoelectric stiffness matrix is denoted by $K_{\phi\phi}$. The matrix A plays a role of computing actuator control force from the applied voltages ϕ_A to actuators, and the matrix S plays a role of computing electrical potentials ϕ_S on sensors from the displacements w.

It is necessary to transform the equations of motions into the state-space form for the aeroservoelastic analysis, and the unsteady aerodynamic forces should be approximated in terms of rational functions of Laplace variable. In this paper, the minimum state method [9] combined with optimization techniques is adopted for the rational function approximation. The minimum state method approximates the aerodynamic influence matrix by

$$\left[\tilde{Q}(\bar{s})\right]=[Q_0]+[Q_1]\bar{s}+[Q_2]\bar{s}^2+[D](\bar{s}[I]-[R])^{-1}[E]\bar{s}, \tag{3}$$

where the non-dimensional Laplace variables (=sb/V) is denoted by s, semi-chord length at the wing root, free stream velocity and the Laplace variable are denoted by b, V and s, respectively. The unknown coefficient matrices are denoted by Q_0, Q_1, Q_2, D, R and E. Physically, Q_0, Q_1 and Q_2 capture the dependence of the unsteady aerodynamics on displacement, velocity and acceleration, respectively. The last term in the right-hand side of Eq. (3) captures the lag in the construction of aerodynamic forces associated with the circulatory effects. As an optimizer, the DFP (Davidon-Fletcher-Powell) variable metric method is adopted with the golden section method in the ADS (Automated Design Synthesis) program [10].

When a modal approach is introduced, the following state-space equations that include the effects of piezoelectric control forces can be obtained from Eqs. (1)-(3):

$$\begin{aligned} \{\dot{x}\} &= [A_S]\{x\} + [B_S]\{\phi_A\}, \\ \{x\} &= \left\{ \{w_m\}^T \quad \{\dot{w}_m\}^T \quad \{p\}^T \right\}^T, \end{aligned} \tag{4}$$

where the system matrix is denoted by A_S and the input matrix is denoted by B_S, which depends on the location of piezoelectric actuators. The state vector is denoted by x, which consists of the modal displacements w_m, the modal velocities and the augmented aerodynamic states p.

B. Optimal Placement of Sensors and Actuators for Measurement and Control of Torsional Vibration

Flutter suppression of composite plate wings based on the measurement and control of torsional vibration with a limited number of sensors and actuators is examined in this research. Here, the measurement and control systems have been constructed by the optimal placement of sensors and actuators based on the minimization criteria of observation and control spillovers for the highly precise measurement and control of torsional vibration.

a) Design of modal transducer based on the optimal placement of sensors and the optimization of sensor gain distribution [11] In this paper, piezoelectric sensors are used as a modal transducer for identifying specific modes in measurement of dynamic aeroelastic response of cantilevered laminated plates. Total output voltage of all sensors Φ_S can be obtained as a sum of each sensor output voltage $\phi_{s,i}$ multiplied by the corresponding sensor gain g_i as follows:

$$\Phi_S(t) = \sum_{i=1}^{ns} \phi_{s,i}(t) g_i = \{\phi_s\}^T \{g\} = -\{w_m(t)\}^T [\Phi]^T [S]^T \{g\}, \tag{5}$$

where the modal matrix is denoted by Φ. Optimization of the sensor gain distribution g_{1T} to construct a modal transducer that estimates the modal displacement of the first torsional mode from electrical potentials on each sensor under a given sensor location can be represented in the following constrained optimization problem [11]:

$$\begin{aligned} &\text{maximize} \quad -\{\phi_{1T}\}^T [S]^T \{g_{1T}\}, \\ &\text{subject to} \quad [\Phi_{1T}]^T [S]^T \{g_{1T}\} = 0, \quad \{g_{1T}\}^T \{g_{1T}\} = 1, \end{aligned} \tag{6}$$

where the modal vector of the first torsional vibration mode is denoted by ϕ_{1T} and the modal matrix which consists of eigenvectors except those of the higher residual modes and that of the first torsional mode ϕ_{1T} is denoted by Φ_{1T}. The optimal sensor gain distribution can be obtained as the eigenvector corresponds to the maximal eigenvalue of the eigenvalue problem, which is equivalent to the optimization problem stated as above. In addition, a modal transducer for the first torsional vibration mode is constructed by the optimal placement of sensors based on the minimization criterion of observation spillover [12]. The optimization problem minimizing the observation spillover can be stated as follows:

$$\text{minimize} \ \lambda_{\max}\left(\{s_{sp}\}\{s_{sp}\}^T \right), \tag{7}$$

where $\lambda_{\max}$ is the maximal eigenvalue of the matrix and s_{sp} represents the relation between the higher residual modes and the observation spillover. From Eq. (7), the sensor locations minimizing the maximal eigenvalue of $\{s_{sp}\}\{s_{sp}\}^T$ become the optimal sensor locations, and then the specific modal displacement $w'_{m,1T}$ is estimated from the output of the sensors optimally placed as follows:

$$w'_{m,1T}(t) = -\frac{\Phi_s(t)}{\{\phi_{1T}\}^T [S]^T \{g_{1T}\}}. \tag{8}$$

b) Optimal placement of actuators for control of torsional vibration [12] In this paper, the LQR with output feedback is applied for a design of flutter suppression system of cantilevered laminated plates with segmented piezoelectric sensors and actuators.

The quadratic performance index is formulated based on the LQR control theory as follows:

$$J = \int_0^\infty \left(\{x\}^T [R_1] \{x\} + \{\phi_A\}^T [R_2] \{\phi_A\} \right) dt \tag{9}$$

where R_1=diag[Ω,I,I] and R_2=rI are the symmetric weighting matrices on states and control inputs, respectively. The matrix with free-vibration eigenvalues on the diagonal is denoted by Ω. The state feedback gain matrix minimizing the quadratic performance index described as Eq. (9) can be obtained by solving the algebraic Riccati equations [13]. An actuation system in order to control the first torsional vibration mode is constructed by the optimal placement of actuators based on the minimization criterion of control spillover [12]. The optimization problem minimizing the control spillover can be stated as follows:

$$\text{minimize } \lambda_{\max}\left([A_{sp}]^T [A_{sp}] \right), \tag{10}$$

where A_{sp} represents the relation between the higher residual modes and the control spillover. From Eq. (10), the actuator locations minimizing the maximal eigenvalue of $[A_{sp}]^T[A_{sp}]$ become the optimal actuator locations.

In the case of that all of the aerodynamic states p and all of the rest modal displacements/velocities except those of the first torsional vibration mode are excluded from the states for feedback purpose, the applied voltages to piezoelectric actuators are determined by the pseudo-optimal output feedback gain matrix K_{FO} obtained based on the minimum norm method [14] as follows:

$$\begin{aligned} \{\phi_A\} &= -[K_{FO}]\{y\} = -[\bar{K}_F][C_s]^T \left([C_s][C_s]^T \right)^{-1} \{y\}, \\ \{y\} &= [C_s]\{x\}, \end{aligned} \tag{11}$$

where the modified state feedback gain matrix to generate control force applied to only the first torsional mode is denoted by $\bar{K}_F$ and the output vector and the output matrix are denoted by y and C_S, respectively.

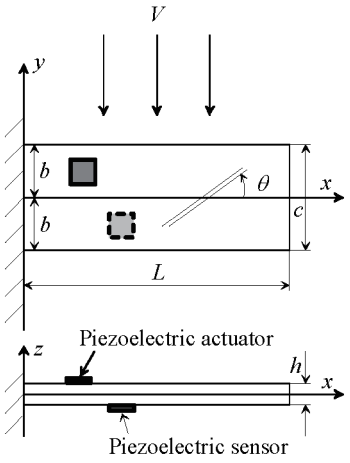

Figure 1 Cantilevered laminated plates (L=305mm,c=2b=76.2mm,h=0.804mm)

III. Numerical Results and Discussions

A. Numerical Model

In this paper, a cantilevered laminated plate $[0_2/90]_s$ with piezoelectric patches shown in Fig. 1 is employed. PVDF sensors and PZT actuators are placed on the bottom and top surfaces of the plate. The material properties of lamina of graphite/epoxy composite, PZT and PVDF patches are shown in Tables 1-3. Here, the in-plane stiffness and piezoelectric characteristics of piezoelectric materials are assumed to be isotropic in this research. The 12x6 and 8x6 elements are used for the structural and aerodynamic analyses, respectively, and the sizes of sensors and actuators are same as that of a finite element in the structural analysis. The eight-node rectangular isoparametric element is employed in the present structural analysis based on Mindlin plate theory. After the vibration analysis, a modal reduction is performed using the lowest eight modes to solve Eq. (1), as shown in Eq. (4), and then the Runge-Kutta method of the fourth order is adopted to integrate the state-space equations described as Eq. (4).

To validate the present aeroelastic analysis, the flutter velocity of cantilevered laminated plates without piezoelectric patches is compared with the reported results [15] in Table 4. This table shows that the present results agree well with the reported experimental results and computational results obtained by the frequency-domain analysis. These

Table 1 Material properties of CFRP

E_{11} [GPa]	E_{22} [GPa]	G_{12}=G_{13}=G_{23} [GPa]	ν_{12}	ρ [kg/m^3]
98.0	7.90	5.60	0.28	1520

Table 2 Material properties of PZT

d_{31}=d_{32} [pm/V]	ε_{33} [nF/m]	E_{11}=E_{22} [GPa]	ν_{12}	ρ [kg/m^3]	Thickness [mm]
254	15.0	63.0	0.30	7600	1.0

Table 3 Material properties of PVDF

d_{31}=d_{32} [pm/V]	ε_{33} [nF/m]	E_{11}=E_{22} [GPa]	ν_{12}	ρ [kg/m^3]	Thickness [mm]
22.0	0.1062	2.00	0.29	1800	0.1

Table 4 Comparison of flutter velocities

Laminate configurations	Flutter velocity [m/s]		
	Present	Ref. [15] Exp.	Ref. [15] Comp.
$[0_2/90]_s$	22.9	25	21.0
$[+45_2/0]_s$	27.6	28	27.8
$[+30_2/0]_s$	27.1	27	27.8

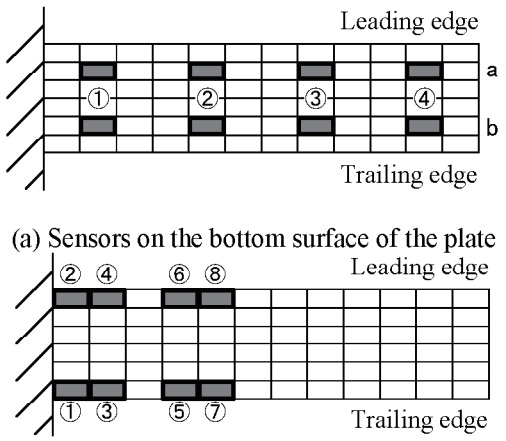

(a) Sensors on the bottom surface of the plate

(b) Actuators on the top surface of the plate

Figure 2 Locations of sensors/actuators

Table 5 Natural frequencies and flutter velocity for $[0_2/90]_s$ laminate (Fig. 2)

Natural frequencies [Hz]					Flutter velocity
First	Second	Third	Fourth	Fifth	[m/s]
14.9	52.4	71.4	124.7	194.0	31.1

results indicate that the present analysis can produce accurate results.

B. Critical Measured and Controlled Modes for Flutter Suppression

At first, critical measured and controlled modes for flutter suppression of a $[0_2/90]_s$ cantilevered laminated plate is examined. The eight sensors and the eight actuators are placed on the bottom and top surfaces of the plate, respectively, as shown in Fig. 2. The natural frequencies of the lowest five modes and the open-loop flutter velocity of a $[0_2/90]_s$ cantilevered laminated plate with sensors and actuators are shown in Table 5. As compared with Table 4, it can be found that the flutter velocity increases due to the mass and stiffness properties of piezoelectric actuators. For an active control design, the design velocity is set to be 34.2m/s and the value of the weighting coefficient r in Eq. (9) is set to be 10^1.

Flutter suppression based on the feedback control on the specific mode, which needs to be controlled among controlled modes and is named as critical controlled mode, and that, which needs to be measured among measured modes and is named as critical measured mode, is examined. Figure 3 shows the results of flutter control based on the second vibration mode, which corresponds to the first torsional vibration mode, at the design velocity. Here, the vibration of the plate is induced by sudden release of 0.1mm initial deflection of the center of the wing tip and the control is started after a lapse of 0.3s in this case. From this figure, it can be found that the divergent vibration can be suppressed by pseudo-optimal output feedback control based on the measurement and control of the first torsional vibration mode. On the contrary, Fig. 4 shows the results of flutter control based on the first or the third vibration modes, which correspond to the lower

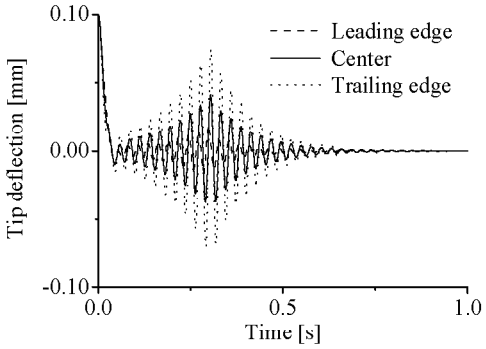

Figure 3 Result of control based on the 1T mode

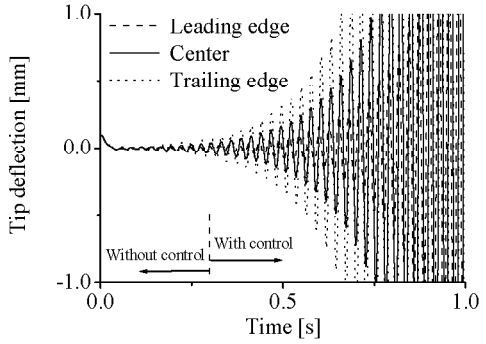

(a) Based on the 1B mode

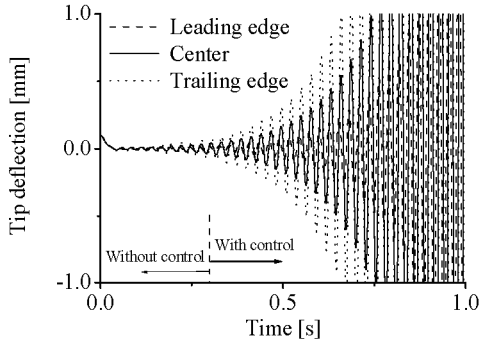

(b) Based on the 2B mode

Figure 4 Results of control

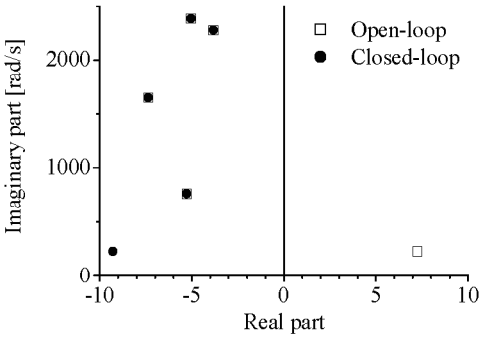

Figure 5 Comparison of open- and closed-loop eigenvalues at design velocity

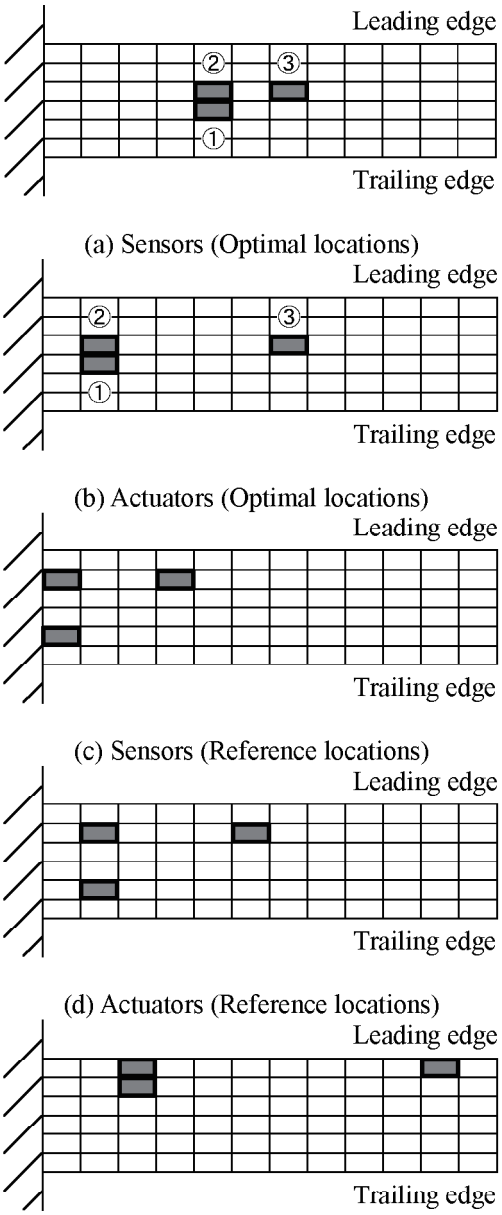

(a) Sensors (Optimal locations)

(b) Actuators (Optimal locations)

(c) Sensors (Reference locations)

(d) Actuators (Reference locations)

(e) Sensors (Optimum for reference locations of actuators)

Figure 6 Locations of sensors/actuators

Table 6 Natural frequencies and flutter velocity for $[0_2/90]_s$ laminate (Fig. 6(a) and 6(b))

Natural frequencies [Hz]					Flutter velocity
First	Second	Third	Fourth	Fifth	[m/s]
11.6	45.9	67.6	144.4	185.1	27.7

Table 7 Optimal values of sensor gain

①	②	③
0.7040	-0.6862	0.1829

bending vibration modes, at the design velocity. From this figure, it is also found that the divergent vibration cannot be suppressed by pseudo-optimal output feedback control based on the measurement and control of the bending vibration mode.

Figure 5 shows the changes in eigenvalues for the open-loop system and the closed-loop system by using feedback control based on the second vibration mode at the design velocity. From this figure, it is found that the present controller makes the open-loop system stable by moving unstable eigenvalue to stable region parallel to real axis, meanwhile the stable eigenvalues in the open-loop system keep their positions. The present controller, that is to say, has no effect on the increase of the fictitious torsional stiffness of plate, but has an effect on the increase of the damping of the first torsional mode of plate. This is also confirmed from the results that a divergent vibration can be similarly suppressed by using the present controller whether the modal displacement of the second vibration mode is included in the feedback variables or not.

These results show that the measurement and control of the torsional vibration mode is essential for flutter suppression of composite plate wings, and a feedback control based on the first torsional vibration mode can suppress the divergent vibration efficiently when using a single vibration mode feedback control scheme.

C. Flutter Suppression based on the Optimal Placement of Sensors and Actuators

In the next examples, a stable flutter suppression methodology of composite plate wings by using a limited number of sensors and actuators is studied. For the highly precise measurement and control of the torsional vibration mode, optimal location of piezoelectric sensors and actuators is searched by the minimization criteria of observation and control spillovers. Here, the optimal locations of sensors and actuators should be determined based on the simultaneous optimal placement, since the stiffness and mass properties of piezoelectric sensors/actuators are considered in the present structural analysis. However, the influence of the sensor locations on the vibration characteristics of composite plate wings can be neglected due to lightweight and high-flexibility of sensor chosen in numerical examples. Therefore, the optimal locations of sensors and actuators are determined successively in this paper.

When three sensors and three actuators are used, the optimal sensor and actuator locations obtained from the criteria in Eqs. (7) and (10) are shown in Fig. 6, respectively. The optimal locations can be determined by a round-robin calculation for all possible combinations of sensor and actuator locations in this paper. It is noted that Fig. 6(c) and 6(d) show a set of different sensor locations and that of different actuator locations, which are chosen arbitrarily and named as reference location. It is also noted that Fig. 6(e) shows the optimal sensor locations obtained from the criterion in Eq. (7) under the reference actuator locations shown in Fig. 6(d). Table 6 shows the natural frequencies and the open-loop flutter velocity for the

cantilevered laminate with sensors and actuators optimally placed as shown in Fig. 6(a) and 6(b). In addition, Table 7 shows the optimal values of the sensor gain for the second mode, which corresponds to the first torsional vibration mode. It should be noted that the fourth ~ eighth modes and the fourth ~ sixth modes are the residual modes in terms of observation and control spillovers in Eqs. (7) and (10), respectively. As for the modal transducer, an Infinite Impulse Response (IIR) low-pass filter of inverse-Chebyshev type with the cut-off frequency of 68Hz, which lies between the third and the fourth natural frequencies, is added in order to stabilize the flutter suppression in the present numerical examples. Here, a modal velocity can be estimated by a finite difference approximation for the values of the estimated modal displacements. For the active control design, the design velocity is set to be 30.5m/s, and the value of the weighting coefficient r in Eq. (9) is set to be 10^1.

Figure 7 shows the results of control at the design velocity. This figure shows the effect of the locations of sensors on the flutter suppression. Figures 7(a) and 7(b) correspond to the deflection of the plate tip controlled by actuators placed on the optimal location as shown in Fig. 6(b) based on the estimated modal displacement by optimal modal transducer and by sensors placed on reference locations as shown in Fig. 6(c), respectively. Besides, Fig. 7(c) shows the control voltages applied to the piezoelectric actuators, which corresponds to Fig. 7(a). In this paper, the vibration of the plate is induced by sudden release of 0.1mm initial deflection of the center of the wing tip and the control is started after a lapse of 0.3s in this case. From this figure, it is found that the optimal modal transducer can suppress the divergent vibration efficiently. On the contrary, it is also found that the vibration diverges quickly due to observation spillover caused by the reference modal transducer. Figure 8 shows the comparison of the power spectrums of the modal velocity of the first torsional vibration mode estimated by the optimal and reference modal transducers. Here, the free stream velocity is the same as the flutter velocity and a low-pass filter is also added. The vibration of the plate is induced by sudden release of 0.1mm initial deflection of the center of the wing tip. From this figure, it can be found that the amplitudes in the fourth ~ sixth vibration modes show remarkable reduction although those in the seventh ~ eighth modes show some increases due to the optimal sensor placement. On one side, the optimal sensor gain distribution plays a role as a kind of modal band-pass filter that passes the first torsional vibration mode in the lowest three vibration modes. On the other side, the optimally located sensors play a role as a kind of modal low-pass filter that passes the lowest three modes, that is to say, the performance of this low-pass filter depends heavily on the sensor location. Since a highly-accurate modal measurement of the

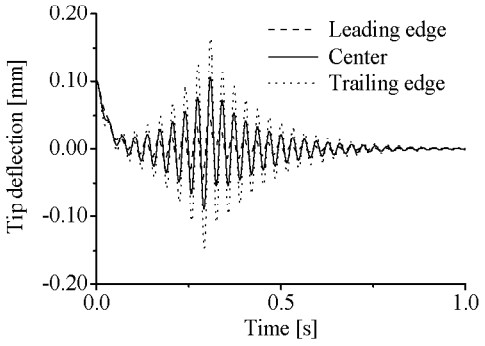

(a) Time histories of tip deflections (Optimal locations of sensors)

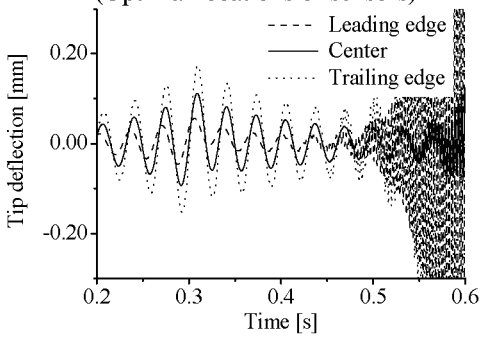

(b) Time histories of tip deflections (Reference locations of sensors)

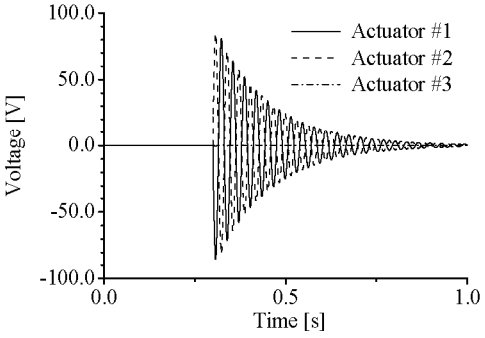

(c) Time histories of control voltages (Optimal locations of sensors)

Figure 7 Results of control

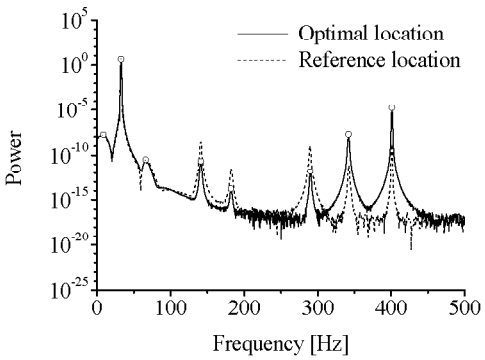

Figure 8 Effect of location of sensors on power spectrum of the modal velocity of 1T mode (V=27.7m/s, with filtering)

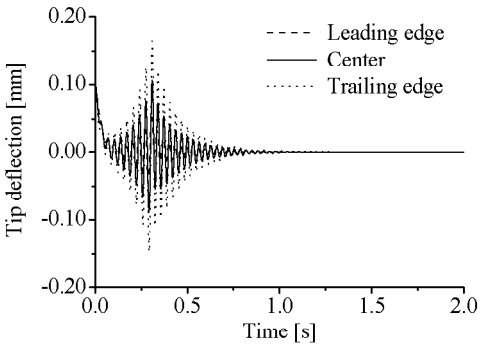

(a) Time histories of tip deflections (Optimal locations of actuators)

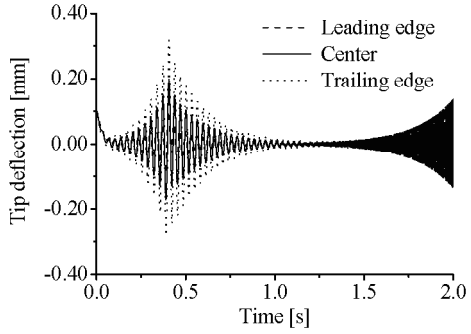

(b) Time histories of tip deflections (Reference locations of actuators)

Figure 9 Results of control

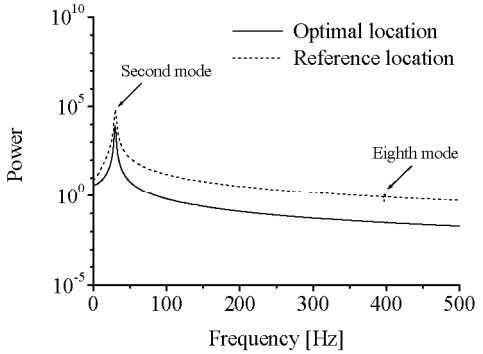

Figure 10 Effect of location of actuator on power spectrum of the modal control force of 1T mode (V=30.5m/s)

modal displacement of the first torsional vibration mode can be realized by a pair of these filter-like elements, it is clarified that the optimal placement of sensors is indispensable to the flutter suppression based on the estimated modal displacement for suppressing observation spillover.

Figure 9 shows the results of control at the design velocity. This figure shows the effect of the locations of actuators on the flutter suppression. Figures 9(a) and 9(b) correspond to the deflection of the plate tip controlled by actuators placed on the optimal location and on the reference locations as shown in Fig. 6(d), respectively, based on the estimated modal displacement by optimal modal transducer. In this case, the vibration of the plate is induced by sudden release of 0.1mm initial deflection of the center of the wing tip and the control is started after a lapse of 0.4s. From this figure, it is found that the vibration converges by control in both cases. The actuators placed on the reference locations, however, cause divergent vibration again due to control spillover after a lapse of about 1.0s. Figure 10 shows the comparison of the power spectrums of the modal control force applied to the first torsional vibration mode in the cases of the optimal and reference actuator locations. Here, the free stream velocity is the same as the design velocity and the exact modal displacement and modal velocity of the first torsional mode calculated by the finite element analysis are used for feedback purpose. From this figure, it can be found that the amplitude in the eighth vibration mode shows considerable reduction due to a highly-accurate modal control for the controlled modes based on the optimal actuator placement. On one side, the output feedback gains play a role as a kind of modal band-pass filter that passes the first torsional vibration mode in the lowest three vibration modes. On the other side, the optimally located actuators play a role as a kind of modal low-pass filter that passes the lowest three modes, that is to say, the performance of this low-pass filter depends heavily on the actuator location, same as modal transducer design. Since a highly-accurate modal control for the first torsional vibration mode can be realized by a pair of these filter-like elements, it is clarified that optimal placement of actuators is indispensable to the flutter suppression based on the estimated modal displacement for suppressing control spillover.

Figure 11 shows the time histories of the deflection of the plate tip controlled by actuators placed on the reference locations as shown in Fig. 6(d) based on the estimated modal displacement by sensors placed on the optimal locations as shown in Fig. 6(e). From this figure, it is indicated that the divergent vibration does not occur immediately after control starts, like that shown in Fig. 9(a). Figures 12 and 13 show the time histories of the measured modal displacement of the second vibration mode and those of the modal control force applied to the fourth vibration mode, respectively. In Fig. 12, it is found that the higher residual modes have an effect on the modal displacement of the second vibration mode after a lapse of about 1.6s in the case of the reference actuator locations. In Fig. 13, it is also found that the higher residual modes affect the modal control force applied to the fourth vibration mode after a lapse of about 1.6s in the case of the reference actuator locations, and makes it diverge gradually, unlike the case of the optimal locations. Therefore, it is clarified again that optimal placement of actuators is indispensable to the flutter suppression based on the estimated modal displacement for suppressing control spillover.

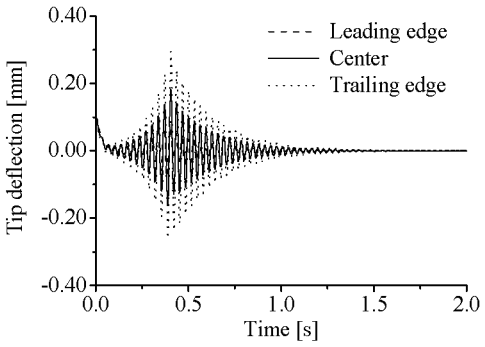

Figure 11 Result of control
(Reference locations of actuators)

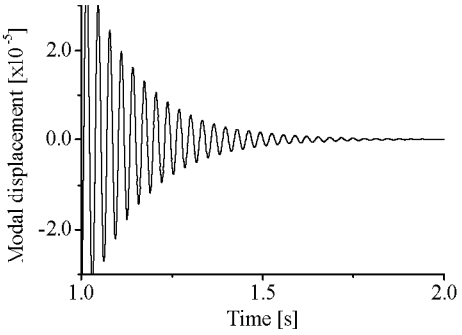

(a) Optimal locations of actuators

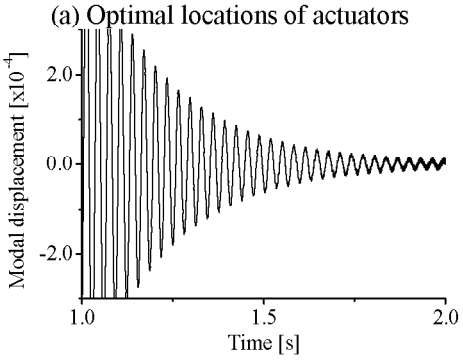

(b) Reference locations of actuators

Figure 12 Time histories of modal displacement of the second vibration mode

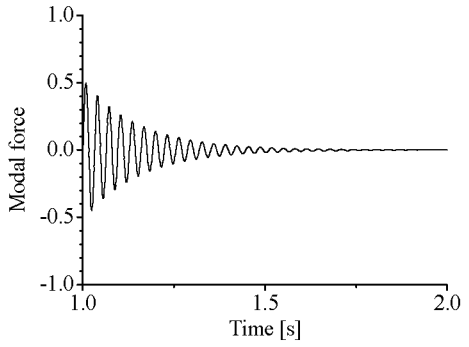

(a) Optimal locations of actuators

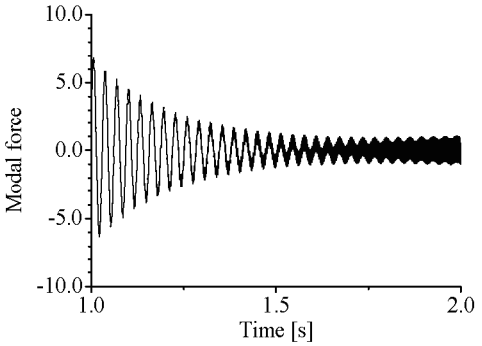

(b) Reference locations of actuators

Figure 13 Time histories of modal control force of the fourth vibration mode

These results show the importance of the locations of sensors and actuators for flutter suppression and that the present method can realize the flutter suppression based on the measurement and control of the first torsional vibration mode by using a limited number of segmented piezoelectric sensors and actuators.

IV. Conclusions

Flutter suppression methodology of cantilevered laminated plates with segmented piezoelectric sensors and actuators has been studied in this paper. Modal transducer for measurement of the modal displacement of the first torsional vibration mode is designed by the optimal placement of PVDF sensors based on the minimization criterion of observation spillover. Actuation system to generate the modal force for the first torsional vibration mode is designed by the optimal placement of PZT actuators based on the minimization criterion of control spillover. It is clarified from the numerical results that flutter suppression of composite plate wings based on the measurement/control of the first torsional vibration mode becomes possible by optimal placement of a limited number of sensors and actuators. In addition, the experimental verification should be needed in the future work.

Acknowledgement

The author would like to thank Dr. Hisao Fukunaga for a valuable discussion.

References

[1] Livne E. Future of airplace aeroelasticity. Journal of Aircraft 2003; 40(6): 1066-1092.

[2] Mukhopadhyay V. Historical perspective on analysis and control of aeroelastic responses. Journal of Guidance, Control, and Dynamics 2003; 26(5): 673-684.

[3] Horikawa H, Dowell EH. An elementary explanation of the flutter mechanism with active feedback controls. Journal of Aircraft 1979; 16(4): 225-232.

[4] Nakamichi J, Yamamoto K, Nakamura T, Ishikawa K, Enomoto S. Research activities in JAXA. Aeronautical and Space Sciences Japan 2006; 54(624): 17-19 (in Japanese).

[5] Giurgiutiu V. Review of smart-materials actuation solutions for aeroelastic and vibration control. Journal of Intelligent Material Systems and Structures 2000: 11(7); 525-544.

[6] Lazarus KB, Crawley EF, Lin CY. Fundamental mechanisms of aeroelastic control with control surface and strain actuation. Journal of Guidance, Control, and Dynamics 1995; 18(1): 10-17.

[7] Crawley EF, de Luis J. Use of piezoelectric actuators as elements of intelligent structures. AIAA Journal 1987; 25(10): 1373-1385.

[8] Ueda T, Dowell EH. A new solution method for lifting surfaces in subsonic flow. AIAA Journal 1982; 20(3): 348-355.

[9] Karpel M. Time-domain aeroservoelastic modeling using weighted unsteady aerodynamic forces. Journal of Guidance, Control, and Dynamics 1990; 13(1): 30-37.

[10] Vanderplaats GN, Sugimoto H. A general-purpose optimization program for engineering design. Computers and Structures 1986; 24(1): 13-21.

[11] Kim J, Hwang JS, Kim SJ. Design of modal transducers by optimizing spatial distribution of discrete gain weights. AIAA Journal 2001; 39(10): 1969-1976.

[12] Sun D, Tong L, Wang D. Vibration control of plates using discretely distributed piezoelectric quasi-modal actuators/sensors. AIAA Journal 2001; 39(9): 1766-1772.

[13] Potter JE. Matrix quadratic solution. SIAM Journal on Applied Mathematics 1966; 14(3), 496-501.

[14] Kosut RL. Suboptimal control of linear time-invariant systems subjected to control structure constraints. IEEE Transactions on Automatic Control 1970; AC15(5): 557-563.

[15] Hollowell SJ, Dugundji J. Aeroelastic flutter and divergence of stiffness coupled, graphite/epoxy cantilevered plates. Journal of Aircraft 1984; 21(1): 69-76.